Annals of Botany **126**: 687–699, 2020
doi: 10.1093/aob/mcaa023, available online at www.academic.oup.com/aob

ANNALS OF BOTANY
Founded 1887

PART OF A SPECIAL ISSUE ON FUNCTIONAL-STRUCTURAL PLANT GROWTH MODELLING

Internal trophic pressure, a regulator of plant development? Insights from a stochastic functional–structural plant growth model applied to *Coffea* trees

Véronique Letort[1,*], Sylvie Sabatier[2,3], Michelle Pamelas Okoma[4], Marc Jaeger[2,3] and Philippe de Reffye[2,3]

[1]Univ. Paris-Saclay, CentraleSupélec, MICS, 91190 Gif-sur-Yvette, France, [2]CIRAD, UMR AMAP, F-34398 Montpellier, France, [3]AMAP, Univ. Montpellier, CIRAD, CNRS, INRA, IRD, Montpellier, France, and [4]Department of Seeds and Seedlings Production, University Jean Lorougnon Guédé, Daloa, Ivory Coast
**For correspondence. E-mail Veronique.letort@centralesupelec.fr*

Received: 20 November 2019 Returned for revision: 20 December 2019 Editorial decision: 4 February 2020 Accepted: 30 July 2020
Electronically published: 5 August 2020

• **Background and Aims** Using internal trophic pressure as a regulating variable to model the complex interaction loops between organogenesis, production of assimilates and partitioning in functional–structural models of plant growth has attracted increasing interest in recent years. However, this approach is hampered by the fact that internal trophic pressure is a non-measurable quantity that can be assessed only through model parametric estimation, for which the methodology is not straightforward, especially when the model is stochastic.
• **Methods** A stochastic GreenLab model of plant growth (called 'GL4') is developed with a feedback effect of internal trophic competition, represented by the ratio of biomass supply to demand (Q/D), on organogenesis. A methodology for its parameter estimation is presented and applied to a dataset of 15 two-year-old *Coffea canephora* trees. Based on the fitting results, variations in Q/D are reconstructed and analysed in relation to the estimated variations in organogenesis parameters.
• **Key Results** Our stochastic retroactive model was able to simulate realistically the progressive set-up of young plant architecture and the branch pruning effect. Parameter estimation using real data for *Coffea* trees provided access to the internal trophic dynamics. These dynamics correlated with the organogenesis probabilities during the establishment phase.
• **Conclusions** The model can satisfactorily reproduce the measured data, thus opening up promising avenues for further applying this original procedure to other experimental data. The framework developed can serve as a model-based toolkit to reconstruct the hidden internal trophic dynamics of plant growth.

Key words: GreenLab, parameter estimation, plant development, Bernoulli random process, functional–structural plant growth model, source–sink balance, trophic competition, *Coffea*.

INTRODUCTION

Development plays a key role in determining the set-up of plant architecture and its growth. It is therefore a core component of most functional–structural plant growth models (FSPMs) (Evers *et al.*, 2018): accounting for plant architecture and its effects on growth is precisely what characterizes an FSPM, in contrast to the so-called crop models or process-based models (e.g. Brisson *et al.*, 2003). Plant development is driven by the iterative and simultaneous activity of the different meristems, at work in each of the growing points of its structure. When described at the organ scale, as commonly done in most FSPMs, plant structure can be conveniently defined as a static set of interconnected organs with a particular topological and geometrical organization; development is thus the dynamic process driving structure evolution throughout plant growth. Diverse formalisms have been used or developed to represent plant structure and development in FSPMs, such as L-systems (Prusinkiewicz and Lindenmayer, 1990), dual-scale automata in the GreenLab FSPM 'series' studied in this paper (Zhao *et al.*, 2001), formal grammars (Kurth and Sloboda, 1999) and graphs (Godin and Caraglio, 1998). Behind this apparent diversity, all these formalisms share common generic properties: they can deal with different spatial scales depending on the application at aim (cell, organ, phytomer, axis, etc.) and they incorporate a way to describe the rules that determine the fate of a bud depending on its position and on its current characteristics. Although not an exhaustive review, we can list the following categories:

(1) Development is determined by deterministic rules given as input, i.e. no plasticity of the plant structure in response to internal variables can be simulated: e.g. GreenLab 'GL1' (Yan *et al.*, 2004; Guo *et al.*, 2006; Ma *et al.*, 2018), L-Peach (Allen *et al.*, 2005) or the model introduced by Coussement *et al.* (2018). This category includes models with deterministic development driven by environmental variables (e.g. Louarn and Faverjon, 2018). Such a development module can be useful as a convenient framework for specific studies at fine scales or of detailed processes (e.g. transport phenomena within the plant structure). Unless taking into account environmental control, the relevance of this deterministic development hypothesis for real applications is limited to a few single-stemmed species (maize: Yan *et al.*, 2004; sunflower: Wu *et al.*, 2012) or to 'average' plant representations, that is to say simulations that represent only the

average structure of sampled plants from a single population (see Lemaire *et al.*, 2009, for an illustration of this approach).

(2) Development is stochastic: using bud outbreak probabilities in the GreenLab model 'GL2' (Kang *et al.*, 2008, 2018; Wang *et al.*, 2010), stochastic L-systems associated with a collision detection algorithm to impede bud outbreak if the position is already filled in LIGNUM (Perttunen *et al.*, 2005), and hierarchical hidden Markov and semi-Markov models in MappleT for which the transition probability matrices are estimated annually (Costes *et al.*, 2008). Here again, environmental variables can be taken into account in these probabilistic frameworks. For instance, in the model by Sterck *et al.* (2005), flush probability depends on phytomer position and daily photosynthetic light intensity. Simulations with stochastic development allow the user to account for the variability within and among individuals, which can be of interest, for instance, when comparing two cultivars or in a breeding context.

(3) Development is deterministic but regulated by a state variable that is assumed to be representative of the vigour of the plant: the assimilate supply to demand ratio in GreenLab 'GL3' (Mathieu *et al.*, 2009), in Evers *et al.* (2010) or in Ecomeristem (Luquet *et al.*, 2006) where it is called the 'index of competition'. The ECOPALM model (Combres *et al.*, 2013) combines an internal trophic competition index and the effect of photoperiod. Within this category one can also include models in which, with a similar philosophy but at a more local scale, bud outbreak is made dependent on the characteristics of its bearing phytomer through some index quantifying local vigour: for instance in LIGNUM (Lo *et al.*, 2001) the number of activated buds is a function of the segment foliage mass of the bearing tree. As soon as such an interaction between development and a functional variable is included, the dynamics of the model become more complex because a feedback loop is at play, which is a well-known feature of dynamic systems theory. However, the widespread use of such feedback mechanism is strongly hampered by the difficulties induced for parameter estimation, because the supply-to-demand ratio is, by definition, a 'hidden' variable that cannot be directly measured.

(4) Development is stochastic and driven by assimilate supply-to-demand ratio: a reference work was published by Pallas *et al.* (2010) for the Greenlab model 'GL4'. In this GL4 model, the plant is considered as a stochastic self-regulating system that can react to exogenous (e.g. environmental stresses that reduce plant production; organ or branch pruning that reduce plant demand) or endogenous (e.g. growth of new branches or fruits that increase demand) influences. Following on from this pioneering work, here we present a more systematic methodology for parameterization of the Greenlab model 'GL4' and define a new sampling strategy for designing an experimental protocol relevant to this methodology.

This study of typology highlights the importance of the variable representing the internal trophic state of the plant in several FSPMs (types 3 and 4). Using this variable as a regulator of plant development, either in a deterministic or in a stochastic way, is appealing as it has an intuitive rationale: raising a new branch by lateral bud outbreak has a cost that the plant should be able to sustain in its biomass budget. One can therefore legitimately examine to what extent this assumption can be considered valid or, at least, to be a reasonable proxy allowing growth dynamics to be reproduced. This question has a long history but is still not fully resolved, and tackling it is hampered by three important bottlenecks: (1) How do we define and quantify the plant internal trophic pressure (local or global allocation process, absolute or relative definition of organ demand)? (2) How do we estimate its value and evolution throughout plant growth by disentangling it from other processes? (3) How do we estimate the parameters of plant development, especially in the stochastic framework? Question (1) represents a modelling hypothesis. In GreenLab, the choice was to use a global allocation process (Heuvelink, 1995) with a dimensionless relative demand computed based on leaf sink strength as a reference. The rationale is that absolute sink strength is generally defined using potential growth rate (e.g. Evers *et al.*, 2010), which can be difficult to measure experimentally. The choice of leaf as a reference is purely arbitrary (but applicable to nearly every plant species) and could be easily changed. It is not our purpose to discuss point (1) further here. Our aims are to propose a methodology to tackle points (2) and (3) in the framework of a new stochastic and retroactive version of the GreenLab model, and to investigate the possible relationship between internal trophic state and plant development by applying this new methodology to a dataset on coffee trees.

The paper is organized as follows: we first present the model version 'GL4', which accounts for plant development as a stochastic process driven by the ratio of biomass supply to demand. The procedure proposed for its parameter estimation is then presented. This procedure is the latest achievement of a continuous long-term study that has tackled the problems of model parameterization for the different versions of GreenLab, from the simplest to the most complex. It uses organ-scale samples and exploits the concept of 'organic series' (Buis and Barthou, 1984), in line with the work presented by Kang *et al.* (2018) but with adaptations to take into account the retroactions between the plant trophic status and its organogenesis. In the Results, after a case study illustrating some emergent properties of the 'GL4' model, the core of the paper is the application of this new methodology to a dataset collected on 2-year-old coffee trees (*Coffea canephora*) grown in the Ivory Coast: the estimated parameters then allow us to reconstruct the source–sink dynamics (Q/D) of the plants and to investigate, for the first time for this species, the existence and shape of the potential dependencies between organogenesis probabilities and this variable. For the sake of consistency and clarity, the model presentation and all illustrations will use virtual young plants that feature the Roux architectural model (Fig. 1) as defined by Hallé *et al.* (1978): the architecture is determined by a monopodial orthotropic trunk meristem subject to rhythmic growth; the branches are plagiotropic and inserted continuously, with no branching delays or apical death of the stem and branches. These assumptions are consistent with the growth patterns of young *Coffea* trees.

MATERIALS AND METHODS

Main equations of the GreenLab model core

As already briefly discussed, the GreenLab model has been adapted to many versions, each corresponding to different modelling objectives (a detailed description of their common base is given by Letort, 2008). Here, we consider its dynamic, discrete and stochastic version with a time step, termed development

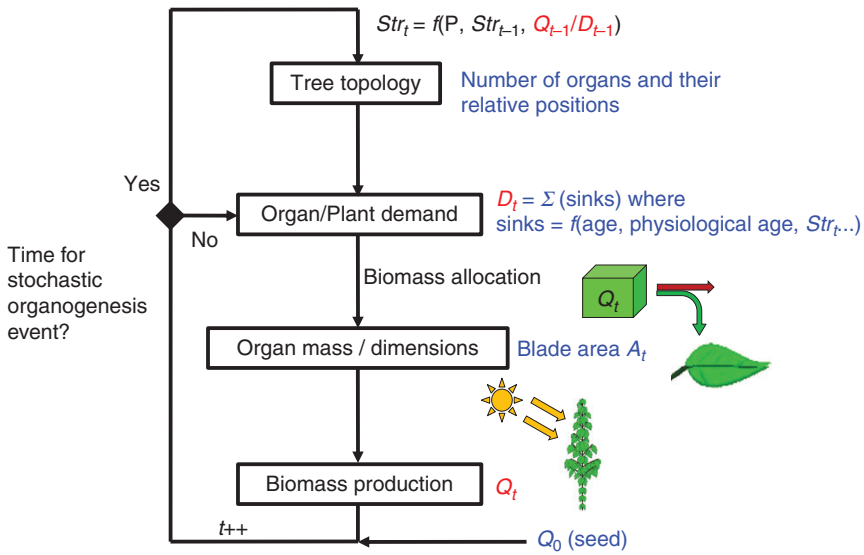

FIG. 1. The dynamic loop of the processes included in the GreenLab model. Plant topology at time t is described by its structure, Str_t, whose formal definition can be based on graph, L-system or dual-scale automation, and updated at each organogenesis event, regulated by stochastic rules and by the ratio of supply to demand as introduced in this paper.

cycle (CD), characteristic of the specific growth dynamics of the simulated species. At a given time, the associated number of CDs can be estimated by fitting the parameters of a binomial distribution to the numbers of phytomers counted on a collection of stems (Kang *et al.*, 2016).

In GreenLab, a deliberately simplified set of physiological phenomena is described, with the aim of representing only the common base to the growth of quasi-all plants whatever the species and of keeping the delicate balance between model complexity, generality and realism (Fig. 1).

Biomass acquisition $Q(t)$ is computed as in eqn (1), based on the formalism of Beer–Lambert's law for light interception, used at the single plant scale as a parametric empirical relationship:

$$Q(t) = E(t) S_p \mu \left(1 - e^{-\frac{S(t)}{S_p}}\right) \quad (1)$$

where $S(t)$ is the sum of the photosynthetically active blade areas at time t; μ is a parameter of light use efficiency that represents the conversion from light energy to assimilate production; S_p is an estimated parameter termed 'production surface' driving the saturation of intercepted light due to self-shadowing or to competition with neighbours. This amount of assimilate is shared between all growing organs o ($o = b$: blades, $o = i$: internodes), regardless of their position (Heuvelink, 1995) and proportionally to their relative demand. Leaf sink strength is chosen as a reference and set to 1. The increment of biomass $\Delta q_o(h,i,t)$ acquired by an organ at age i and branching order h at growth cycle t is then:

$$\Delta q_o(h,\ i,t) = P_o(h)\, \varphi_o(i;\ \alpha_o,\ \beta_o,\ T_o)\, \frac{Q(t-1)}{D(t)} \quad (2)$$

where $D(t)$ is total plant demand, namely the sum, over all plant organs and compartments, of their respective demands. The demand of expanding organs is defined as the product of a sink strength parameter $P_o(h)$ ($h = 1, 2$ in this paper's illustrations) and a sink variation function $i \mapsto \varphi_o(i;\alpha_o,\ \beta_o,\ T_o)$, defined on $\mathbb{R} \to [0, 1]$, that can take for instance the form of a normalized beta density law (Yin *et al.*, 2003) of parameters α_o and β_o whose support is included in $[0, T_o]$. A particular formalism is used for ring growth demand, which is calculated at the global scale as a function of $N_a(t)$ (the number of active leaves at time t in the tree), with reference to the so-called 'pipe-model' theory (Letort *et al.*, 2008; Lehnebach *et al.*, 2018):

$$D_r(t) = P_r \cdot N_a(t) \quad (3)$$

where P_r is the sink value for ring growth. Once globally allocated, the biomass for ring growth is then spread along each internode proportional to the number of active leaves located above its position in the plant architecture. Leaf area is determined from the amount of allocated biomass through an allometric relationship involving a thickness parameter e. This parameter is estimated from a linear regression between leaf area and leaf mass. Note that the root compartment is omitted here for the sake of clarity but could be easily included. The simulation is initialized by $Q(0)$, the biomass provided by the seed at emergence.

Introducing the assimilate supply-to-demand ratio as a key state variable with feedback effect on organogenesis

In eqn (2), it is clear that the ratio of biomass supply to demand $Q(t-1)/D(t)$ is a key state variable of the plant seen as a dynamic system. This ratio can be interpreted as an indicator of the internal state of trophic competition within the plant.

Based on both Kang *et al.*'s (2008) 'GL2' in their stochastic version without feedback of plant physiology on organogenesis and Mathieu *et al.*'s (2009) 'GL3' in their deterministic version with feedback, we introduce here the hypothesis that the

probabilities of phytomer emission from respectively apical and lateral buds depend on the ratio of assimilate supply to demand, *Q/D*. Thus, two parameters of the original stochastic version of the development model, as presented by Kang *et al*. (2016, 2018) and noting that, in our simplified illustration, meristem mortality is not considered, are modified into functions of *Q/D* instead of being fixed as input:

- $a_{h,t} \leftarrow f(Q/D(t),\ K_a(h))$: the probability of branch appearance at branching order h ($h \leq 2$ in this case), at time t, with K_a a vector of associated parameter values
- $b_{h,t} \leftarrow f(Q/D(t),\ K_b(h))$: the probability of phytomer emission along an axis at branching order h, at time t, with K_b a vector of associated parameter values

Several forms could be considered for these functions that take their values in [0, 1], a first natural choice being the sigmoid form, widespread in many biological processes, for instance under the form:

$$b_{h,t}\left(\frac{Q}{D},\ K_b(h)\right) = \frac{K_b \cdot Q(t-1)/D(t)}{1 + K_b \cdot Q(t-1)/D(t)} \tag{4}$$

where in this instance the vector K_b is of dimension 1 and the index h has been omitted for the sake of clarity. For the branching probability a, the same function form is set, with parameter K_a, with $K_a = 200$ arbitrarily chosen to accentuate the base effect presented in our simulated case study, for illustration purposes (see Results for the definition of the base effect). Of course in this simulation study this choice is purely user-defined and an adequate function shape will need to be thoroughly investigated when applications to real plants are considered.

Formally, the development model can therefore be written under the form of a F0L-System [as introduced for GreenLab by Loi and Cournède (2008); see also Diao *et al.* (2012) for the formal description of the production rules in the stochastic model of *Eucalyptus* development) with conditions for the application of the production rules.

Although seemingly insignificant, this modification implies some changes in the simulation loop. Indeed, assuming that the plant has been simulated until time $t-1$, the demand of the next time step is now computed as follows:

- Compute the demand of organs and compartments that were created at previous time steps, $D_{\text{prev}}(t)$ (their demand being zero if they have already finished their expansion phase).
- Track every phytomer bearing functional buds and compute the demand $P_{\text{phyt}}(h(bud),\ 1)$ of the phytomer that might emerge from this bud, weighted by its probability of appearance$\pi(bud,\ Q/D)$: phytomers that have very low probability of appearance will thus have less impact on this 'potential' demand.
- The demand is thus the solution of the following equation:

$$D(t) = D_{prev}(\mathrm{t}) + \sum\nolimits_{bud} \pi(bud,\ Q/D) \cdot P_{phyt}(k(bud),\ 1) \tag{5}$$

which has to be solved either analytically (but tractable only in very simple cases) or numerically using the Newton algorithm. For young plants with the Roux architectural model (presented in the Results), π takes the values:

$$\pi\left(bud, \frac{Q(t-1)}{D(t)}\right) = \begin{cases} \frac{K_b(1)\cdot\frac{Q}{D}}{1+K_b(1)\cdot\frac{Q}{D}} & \text{if bud is apical on main stem} \\ \frac{K_b(2)\cdot\frac{Q}{D}}{1+K_b(2)\cdot\frac{Q}{D}} & \text{if bud is apical on branch} \\ \frac{K_a(2)\cdot\frac{Q}{D}}{1+K_a(2)\cdot\frac{Q}{D}} \cdot \frac{K_b(2)\cdot\frac{Q}{D}}{1+K_b(2)\cdot\frac{Q}{D}} & \text{if bud is lateral} \end{cases} \tag{6}$$

- Using this value of $D(t)$, determine for each bud whether it breaks to create a new phytomer drawn by random with probability $\pi\left(bud, \frac{Q(t-1)}{D(t)}\right)$
- Re-compute the effective value of the demand, taking into account only the phytomer that appeared.
- Allocate biomass to each organ.

A new methodology for model parameterization and experimental sampling

De Reffye *et al.* (2018) presented a new methodology for parameter estimation of the 'GL4' model and tested it on virtual data. The method relies on a series of average measured organ weights to estimate simultaneously both functional (sinks, efficiency, etc.) and topological parameters (K_a, K_b). This *in silico* exercise allowed them to test the method because the exact solution was known and could be compared with the obtained estimates. The number of plant samples could also conveniently be varied, while this is obviously not possible with real experimental data. In summary, they observed that the average of N stochastic simulations converged towards the theoretical average plant computed with the potential structure using the same parameter values when N increased. They found that the model parameters could be satisfactorily estimated using the procedure described above and that the parameters K_a and K_b showed the highest bias. This is logical, as their estimation relies on the fact that information regarding plant development is embedded in data for organ mass, owing to the influence of plant development on its functioning. The results of this necessary *in silico* step now allow us to consider its application on real data.

As this is the first study to investigate the dependency between the internal trophic state of the plant (quantified by the *Q/D* ratio of GreenLab) and the organogenesis probabilities $a_{h,t}$ and $b_{h,t}$ of coffee trees, there was no *a priori* available knowledge on the shape of this dependency. The homographic functional family introduced in eqn (6) was purely arbitrary, and used for illustration purposes only. Therefore, our objective is here to first extract empirical information on the shape of this functional dependency. To this end, we applied the following procedure:

1. Estimation of development parameters by the 'crown analysis' method, as in the GL2 model
2. Estimation of physiological parameters from organic series
3. Reconstruction, throughout the growth process, of the evolution of demand and supply and therefore that of the trophic pressure *Q/D*
4. Examination and discussion of the possible existence of a functional relationship that would consider the *Q/D* ratio as a determinant of the variations of development probabilities throughout plant growth.

5. Simulations of the full model with retroaction terms and its evaluation.

The first two points correspond to the parameter estimation procedure as detailed below.

Regarding step 1, the methodology of 'crown analysis' developed in the 'GL2' model for constant probabilities is presented by Diao *et al.* (2012) for young eucalyptus and by Kang *et al.* (2016) in a theoretical study. Using this method, the probability values of the organogenesis model are estimated based on counts of phytomers at each position in the architecture: the probability of branch appearance (a), the development probability for the stem (b_1) and branches (b_2) as well as the rhythm ratio between them (w). The rhythm ratio parameter describes the deterministic part of the ratio of the rate of phytomer emission on branches to the rate of phytomer emission on the trunk (in practice the effects of parameters w and b_2 can be disentangled via the estimation procedure). The term 'crown' indicates that the analyses and experimental sampling must be done using the tips of axes as origin points. In 'GL4', the probability of branch appearance and the development probability for the branches, denoted a_k and $b_{2,k}$, can vary with their rank k because they depend on Q/D. We present below the associated equations, adapted to take into account this variation.

It can be shown that for N_k the number of phytomers on a branch at rank k from the top:

$$\mathbb{E}(N_k) = w \cdot \frac{k}{b_1} \cdot b_{2,k} \tag{7}$$

$$V(N_k) = w \cdot \frac{k}{b_1} \cdot b_{2,k}(1 - b_{2,k}) + (w \cdot b_{2,k})^2 \cdot \frac{k \cdot \ (1 - b_1)}{b_1^2} \tag{8}$$

The mean and variance in eqns (7) and (8) can be estimated using the experimental dataset consisting of phytomer counts on a collection of stems and their sets of first-order living branches, indexed by the position of the branch from the top (rank k). The system can thus be solved to obtain estimates of $b_{2,k}$ and w. The probabilities of branch appearance $a_{2,k}$ (hereafter simply noted a_k because there is no higher branching order) are estimated as the ratio of the number of branches observed at rank k (their average age being k/b_1) to the total number of positions, $2N_T$. If there are branches of higher order, the same procedure is sequentially repeated for each pair of successive branch orders (Diao *et al.*, 2012).

In step 2, the parameters of the functional part are estimated (sinks and source parameters) from the organic series, using a two-stage Aitken estimator as presented by Cournède *et al.* (2011) based on the generalized least-squares method. This step is unchanged from the work of Kang *et al.* (2018) so we briefly recall here its main principles, for the sake of self-consistent understanding of our paper. The main difficulty for this step is that, because of the stochasticity of plant development, the real age i of a phytomer at rank k from the axis tip is not known (the only information available is that we have $k \le I \le t$, t being the age of the plant). Besides, when several plant samples are measured that do not all share the same topology, the question is to determine how to aggregate these different measurements. To this end, the strategy presented by Kang *et al.* (2018) consists of averaging weights of organs sorted according to their rank k from the axis tip. The resulting sequence is called stochastic topological organic series $\left(\overline{q_o(k,t)}\right)_{1\le k\le t}$ (Fig. 2). The main idea is then to construct an equivalent average theoretical simulated plant that can match the measurements in the optimization procedure for parameter estimation. To this end, we define the potential structure as the union set of all possible structures: it corresponds to the plant structure that would grow if all the probability values were set to 1. Each phytomer of this structure is assigned a real value corresponding to its probability of existence, as illustrated in Fig. 2.

This potential structure allows us to compute the theoretical demand of the potential average plant:

$$D^{\theta}(t) = \sum_{id} \pi(id) \cdot P_{phyt}(h(id),\ age(id)) \tag{9}$$

where the summation is performed over all phytomers of the potential structure arbitrarily indexed by an integer id. The superscript index θ is used here for to indicate variables corresponding to the theoretical average plant that can be computed using the random processes defining the architectural rules. The term $\pi(id)$ represents the probability of existence of phytomer id of physiological age $h(id)$ and $P_{\text{phyt}}(h(id), age(id))$ is its associated demand. An example of these probability values $\pi(id)$ obtained for our Roux model illustration is given in Fig. 2.

By applying the usual GreenLab equations, the theoretical biomass $q_o^{p,\theta}(i,\ t)$of each organ of age i of the potential structure in the plant of age t can be deduced. Superscript p indicates that the 'potential' structure is considered, that is to say the plant with the maximum possible number of phytomers (obtained if they all had a probability of existence equal to 1). The final step is computation of the topological organic series: the average organ weight at rank k in the potential structure is expressed as:

$$q_o^{\theta}(k,t) = \frac{\sum_{i=k}^{t} \pi_{age}(k,i) \cdot q_o^{p,\theta}(i,\ t)}{\sum_{i=k}^{t} \pi_{age}(k,i)} \tag{10}$$

where t is plant age and $\pi_{age}(k,i)$ is the probability that the chronological age of a phytomer of rank k from the tip is i, computed from a truncated negative binomial distribution (k, b). This simulated output can be compared to the vector of averaged measured values stored in the stochastic topological organic series, $\left(\overline{q_o(k,t)}\right)_{1\le k\le t}$.

The model and the methods for parameter estimation were implemented in MATLAB version R2012b and are available on request.

Data acquisition

An experimental study was undertaken at the Divo research station at the National Research Centre for Agronomy (CNRA, 5°46′04.07″N, 5°13′22.09″W) in central western Ivory Coast. This experiment was conducted under common field conditions. Average relative air humidity is ~80 %, average annual rainfall is between 1100 and 1400 mm, and mean temperature ranges between 28 and 32 °C. The 6-month-old seedlings were planted in July 2015 with a spacing of 1.50 m and 3 m between the lines. Fifteen 2-year-old coffee trees (*C. canephora*) were

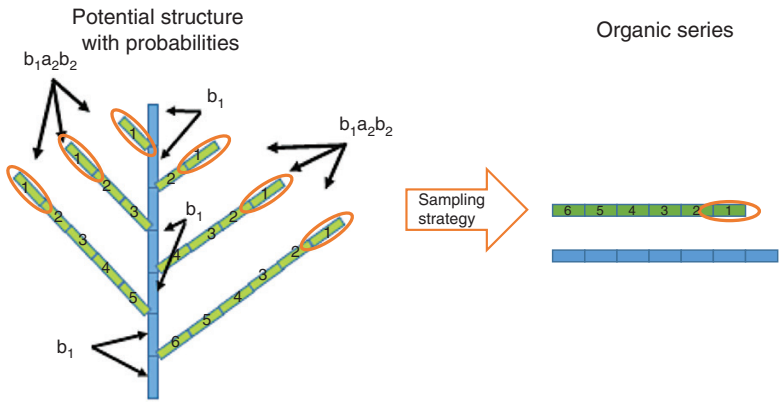

FIG. 2. The concept of potential structure and its application to a plant featuring the Roux architectural model with branching and phytomer appearance probabilities. The sampling strategy is illustrated: organs from the same rank and branching order are pooled together to build the organic series.

measured. At this stage, no branch mortality nor flowering was observed. All plants were described phytomer by phytomer (i.e. a segment of the shoot, which includes an internode, the leaf and axillary buds). The number of phytomers was recorded for each branch, starting from the top of the main stem. The absence or presence of branches on the trunk and their positions were noted. Plant topology was recorded following the Multi-scale Tree Graph (MTG) formalism (Godin and Caraglio, 1998) and analysed using Xplo software (Griffon and de Coligny, 2014, http://amapstudio.cirad.fr/). For each phytomer, the length of the underlying internode, the diameter in the middle of the internode and the presence of branches were measured. We recorded the number of leaves, their length and width. The dry weight of each phytomer (stem and leaves were separated) was recorded (dried at 100 °C for 48 h).

RESULTS

Case study 1: simulating the base effect

Some interesting emergent properties can be simulated with the model. In this first case study, we consider simulation of the base effect during the young growth stages of trees. The base effect is generally due to a phase of primary biomass investment to the root system rather than to the aerial part. It is defined as the progressive set up of the architectural unit and, in our example of the Roux model, is characterized by few and sometimes short-lived branches at the base of the main stem, followed by branches that are progressively more vigorous and numerous (Barthélémy and Caraglio, 2007).

In this virtual experiment, we arbitrarily set the parameters to their values listed in the caption to Fig. 3. Simulations were run for a population of 50 plants with the Roux architectural model until 30 CDs. Figure 3 presents the variations of the average branching probability $a(Q/D)$ with time ± the standard deviations computed over those 50 simulations: the base effect can clearly be observed on the simulated trees with a first zone without branches, then a progressive increase in branch number at older growth stages. This effect is directly related to variations in the supply-to-demand ratio (see Fig. 4C for the Q/D ratio and Fig. 4E for the evolution of biomass production). The slight decrease at time step 11 is caused by the appearance of branches at that time for a large number of plants, leading to a sharp increase in demand and consequently this temporary slowdown in growth as a feedback effect. Once the quasi-equilibrium state is reached, the development probabilities become quasi-constant and the model is thus equivalent to a purely stochastic model without feedbacks.

Case study 2: simulating the effect of branch pruning on phytomer emission probability

Another interesting emergent property of the model is the effect of branch pruning on the rhythm of phytomer emission on the main stem of a monopodial plant. In a dedicated experiment on six different *Coffea* species, Okomas (2018) estimated the phytomer emission probabilities for plants with systematic branch pruning treatments (b_1^p)and for a control plant population (b_1^c), respectively: *C. canephora* ($b_1^p = 0.910.91$, $b_1^c = 0.88$ 0.88), *C. dewewrei* ($b_1^p = 0.920.92$, $b_1^c = 0.770.77$), *C. liberica* ($b_1^p = 0.950.95$, $b_1^c = 0.770.77$), *C. stenophylla* ($b_1^p = 0.890.89$, $b_1^c = 0.780.78$), *C. pseudozangebarie* ($b_1^p = 0.790.79$, $b_1^c = 0.8$ 0.8) and *C. racemosa* ($b_1^p = 0.910.91$, $b_1^c = 0.70.7$). These results indicate that, except for *C. pseudozangebarie*, pruning involves not only larger organs but also a faster development of the stem.

Our hypothesis is that this might be the result of a decrease in the trophic pressure within the plant, which can be simulated owing to its dependency on the supply-to-demand ratio.

Using the same simulation specifications as in the previous paragraph, we performed 50 stochastic simulations until age 30 CDs to compare the growth of plants featuring the Roux architectural model with plants virtually submitted to a total pruning treatment of all lateral branches (therefore featuring a Corner architectural model). The values computed over those 50 simulations are presented in Fig. 4 for, respectively, the probability of phytomer appearance on the main stem (Fig. 4A), supply-to-demand ratio (Fig. 4C), biomass production (Fig. 4E) and mass of the organic series (series consisting of the average mass of organs that share the same characteristics, namely here same rank and branching order) along the main stem, aligned

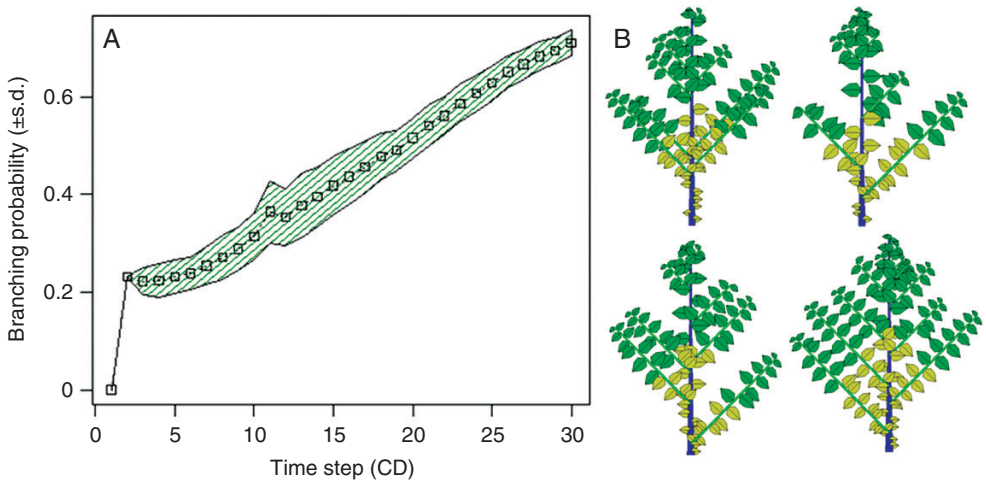

FIG. 3. (A) Variation in branching probability with time in the population of plants with the Roux architectural model: mean values of the 50 stochastic simulations are given with error bars representing ±s.d. in the hatched area. (B) Graphical illustrations of a sample of simulated plant topologies showing the base effect in their early development stages. Values of model parameters, using the notations defined in eqns (1)–(8) are: durations of organ expansion and leaf activity are constant (T = 10 CD), all organs have constant demand (P = 1, α_o = 1, β_o = 1), a density of 5 plants per m^2 that generates some competition pressure from neighbouring plants (S_p = 2000), efficiency parameter μ = 1/30; e = 0.05 g cm^{-2}. A constant environment is fixed with $E(t) = 1^{1\forall t}t$. The parameters of stochastic topological development are branching probability $a\,(Q/D) = \frac{200(Q/D)}{1+200(Q/D)}$ and phytomer appearance probability $b(Q/D) = b\,(Q/D) = \frac{Q/D}{1+\ Q/D}$ (same value for trunk and branches). The maximum life span of branches is not stochastic here and is fixed at 20 CDs.

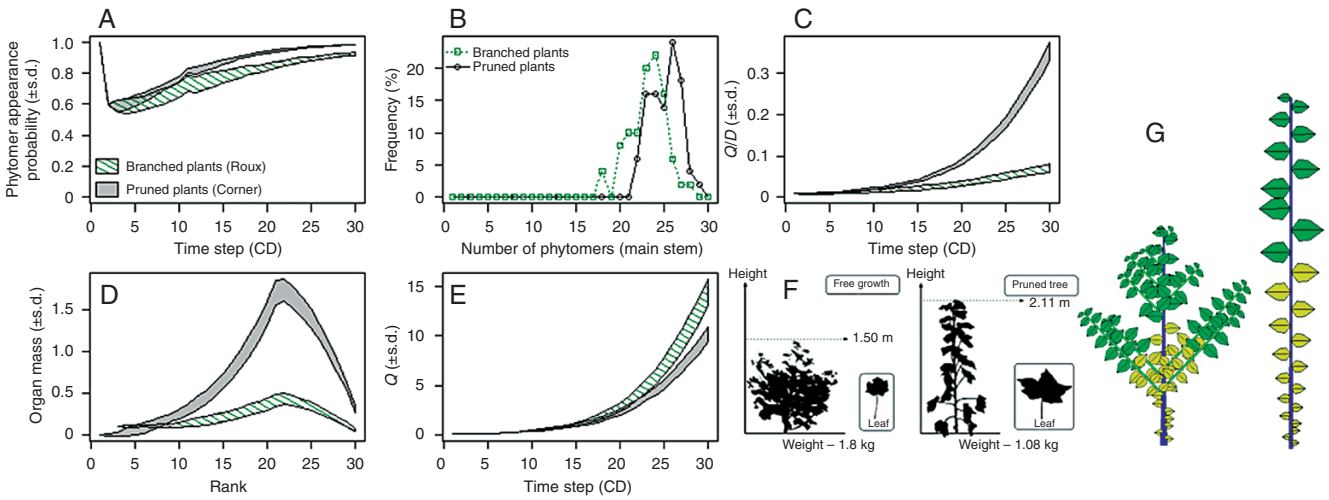

FIG. 4. Virtual pruning experiment using the stochastic GreenLab model with feedback of plant functioning on organogenesis. For each of the two treatment groups (control or pruned): (A) average phytomer appearance probability – at emergence of the axis, the value 1 is fixed for the first CD in order to impose that the axis effectively appears; (B) distribution of the number of phytomers on the main stem (%); (C) evolution of the average ratio of biomass supply to demand; (D) organic series (profile of organ mass) along the main stem according to their rank; (E) evolution of average biomass supply for the two architectures. (F) Visual comparison between branched and pruned cotton plants (source: de Reffye *et al.*, 1999). (G) Illustration of two individuals with maximal (potential) topology. The parameter values are given in the caption to Fig. 3.

at their tips (Fig. 4D). The variance in these variables in the population is not particularly important: the standard deviation represents only a few per cent of the average. This can be explained by the fact that, due to the choice of the Beer–Lambert equation for the production equation, plant topology has a limited impact on its functioning (Letort *et al.*, 2010, 2012): the evolution of biomass supply is similar for the two architectures, with a relative difference of 14.5 % in average simulated duration. The 'base effect' presented in case study 1 explains that there is nearly no difference between the two populations at the beginning of growth. Figure 4 shows that the average supply-to-demand ratio is larger in the pruned plant group, as expected given that they experienced a reduced internal tropic competition due to a reduction in their demand. Therefore, the phytomers on the main stem are clearly larger in the pruned group (Fig. 4D) and they are also more numerous: note that on the graph, the phytomers have been aligned from the axis tip so the ranks at the main stem base are empty for the branched plants that have fewer phytomers. Indeed, the associated mean values of phytomer emission probability on the main stem, $b_1(t)$, are correspondingly larger in the pruned group: it stabilizes at an average of 0.97, vs. 0.92 for branched trees

(Fig. 4A). In turn, this results in a distribution of phytomer number on the main stem that is shifted towards higher values for pruned plants (Fig. 4B), a trend consistent with the observations reported above. Visual representations of the plant shapes are displayed to illustrate the adequacy of this virtual case study to real observations (Fig. 4F, G).

Illustration of the whole estimation process on real experimental data and investigations on source–sink ratio influences

Results of the crown analysis step. The method of crown analysis, as briefly recalled in the previous section, was applied to the coffee dataset. Figure 5 presents in a schematic form the topology of four different trees out of the 15 measured, illustrating the variability in their development. Some branches are always missing at the bottom and the ramification rate increases with plant age. In this first step, this observed variability is assumed to be simply driven by stochastic events with constant or varying probability rates that have to be estimated.

Figure 6A shows the variability of the number of phytomers of the branches located at rank k below the top of the trunk. Based on eqns (7) and (8), the values of phytomer emission probabilities for the trunk ($b_1 = 0.88$) and the lateral axes ($b_2 = 0.93$, this average value is obtained considering all branches pooled regardless of their rank) as well as the rhythm ratio between branches and trunk ($w = 0.9$) are computed. Because the values of b_1 and b_2 are similar, they are considered identical in the simulations below.

A bottom-up analysis of the progressive implementation of the branching makes it possible to quantify the branching rate evolution on the ranks of the trunk phytomers (Fig. 6B). The increase in the rate of branching observed is close to linear, up to rank 14 at which it stabilizes to a constant value of 1. Fitting of a power function to these data gives:

$$a(x) = \left(\frac{x}{14}\right)^{1.25} \text{ if } x \leq 14$$

$$a(x) = 1 \text{ if } x > 14 \qquad (11)$$

These development parameter estimates now makes it possible to compute the rate of realization of phytomers in the potential structure at any position, as represented in Fig. 2. The average production of phytomers resulting from this stochastic development at 27 CDs is $N_1 = 24$ for the trunk and $N_2 = 261$ for the branches.

Results of the organic series analysis. Some model parameters can be directly extracted from observations: the duration of photosynthetic activity of the leaves $t_a = 10$ CDs, the expansion duration of the leaf and internodes $t_x = 4$ CDs. Average specific leaf area, a proxy for leaf thickness, is $e = 0.0095$ g cm^{-2}. We consider a normalized environment with radiation $E = 1$ at each CD. This strong modelling assumption amounts to considering the average environmental conditions throughout tree growth. This is reasonable here as our objective with GreenLab is not detailed exploration of the environmental influences on plant growth (which would be challenging to decipher for growth in open conditions) but rather representation of the main dynamics of growth.

The values for hidden parameters are presented in Table 1 and the graphs comparing simulated to observed data are given in Fig. 7. The higher variability of data points for the base of the branches is due to the fact that the means are computed over a decreasing sample size (older phytomers are less numerous because branches are aligned from their tips and longer axes are less probable).

Reconstruction of the trophic dynamics during coffee growth. Using the estimated parameter values, simulations provide in-depth insights into the growth dynamics. Fitting of the model on the organic series allows us to simulate supply and demand at each growth cycle (Fig. 8). After a first exponential phase, the demand increase slows down and becomes linear. Biomass produced at each time step exhibits a sigmoidal shape. The saturation effect is generally considered as being due to self-shadowing of leaves and to competition with neighbouring trees (density is about one plant per m^2). Note that the development and growth observed on these coffee trees is for a relatively short period (27 CDs correspond to 2 years).

We can now examine the ratio of supply to demand, *Q/D*, in Fig. 8C. The curve irregularity at CD 10 corresponds to the first fall of the oldest leaf. It is thus an artefact of the model due to the fact that leaves abruptly cease contributing to production while in reality the process is of course smoother. In the first phase, *Q/D* progressively increases, which corresponds to the establishment of plant architecture, with a gradual increase in organ size and the appearance of first branches. The subsequent decline in the second phase is due to the increase in demand while production reaches saturation. Interestingly, *Q/D* reaches a maximum at about CD 15, close to the time when branching probability stabilizes. This is now investigating in more detail.

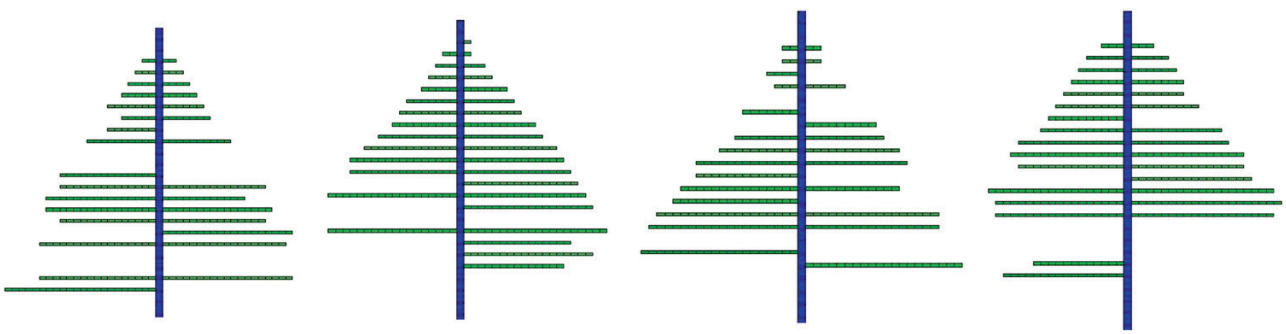

FIG. 5. Schematic representation of four coffee tree crowns among the 15 plants measured.

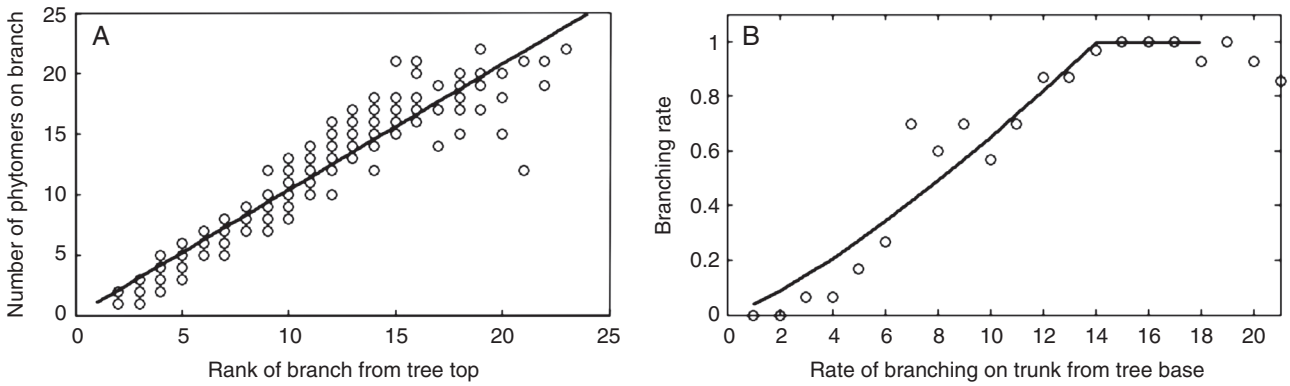

FIG. 6. (A) Variability in the number of phytomers of the branches located at rank k below the top. (B) Evolution of the branching rate from the base of the tree. Lines represent the simulated values.

TABLE 1. *Estimated parameter values (with their estimated standard deviation values). The reference value for sink values is that of leaf of the trunk, set to 1. Due to practical non-identifiability, and without loss of generality, only one parameter of the beta density function was estimated. The other one was empirically fixed.*

Symbol	Name	Estimated value
R (= 1/μ)	Efficiency (inverse)	164.1 (13)
Sp	Saturation parameter	6417 (939)
Q_0	Seed biomass	8.3 (2.1)
$P_a(1)$	Leaf sink on trunk	1 (reference)
$P_a(2)$	Leaf sink on branches	1 (0.06)
$P_i(1)$	Internode sink on trunk	5.2 (3.6)
$P_i(2)$	Internode sink on branches	0.77 (0.4)
Pc	Sink for ring growth	0.2 (0.02)
α_i	Beta density function parameter 1 for internodes	2.8 (1.1)
β_i	Beta density function parameter 2 for internodes	6 (fixed)
α_a	Beta density function parameter 1 for leaves	1.7 (0.36)
β_a	Beta density function parameter 2 for leaves	2.5 (fixed)

Influence of growth on development parameters. Results from Figs 6 and 8, once combined, allow us to investigate the relationship between internal trophic competition, represented by Q/D, and development probabilities. In Fig. 9A, a clear increasing relationship is observed for branching probability, with two successive quasi-linear phases separated at the point corresponding to the first leaf fall. To maintain a unique relationship, it was fitted by a power function, giving:

$$a(x) = 23483x^{5.61},\ R^2 = 0.95 \quad (12)$$

Note that only the data from the establishment phase were included in the regression, because for subsequent values, the probability of branching was consistently equal to 1 although Q/D decreased.

The same type of analysis was performed for the probability of phytomer emission, using the values $b_{2,k}$ estimated from eqns (7) and (8) (Fig. 9B). The rhythm ratio w is kept constant. Only those points corresponding to large enough sample of branches ($n > 15$) were kept, which excluded most basal branches. The points are more dispersed so the linear regression should be considered as indicating a global trend:

$$b(x) = 1.72x + 0.64,\ R^2 = 0.52 \quad (13)$$

Recalculation of demand and biomass with trophic pressure. Equations (12) and (13) allow us to compute the parameter values for branching and development probabilities as functions of the trophic pressure Q/D at each CD. They were introduced in the model and the resulting complete simulations were compared to previous ones (those without a feedback effect of Q/D on the development probabilities) in Fig. 10 for plant demand (Fig. 10A), biomass production (Fig. 10B) and organic series (Fig. 10C). The agreement is good for production and demand as well as the organic series of leaves. For internodes a slight divergence appears at the stem base, which is essentially due to the calculation of secondary growth.

DISCUSSION

Use of Q/D *ratio as a regulating variable*

This work investigated, for the first time, the possible use of internal trophic competition as a regulator of plant development in the GL4 GreenLab model using the 'crown analysis' method to guide our sampling strategy. Following the *in silico* study by De Reffye *et al.* (2018), the model was tested on a real dataset from 15 coffee trees.

The estimation procedure can be considered as globally satisfactory with good adjustment between observed and simulated data for the organic series in Fig. 7. Although this does not prove the validity of the model, it is an encouraging sign for assuming that the trophic dynamics generated by the model are consistent with real dynamics throughout the plant life. Clearly some remaining discrepancies can be tackled, such as the dramatic effect of first leaf fall on biomass production, but we consider that the global trends are interpretable, which is our goal in this study. The same precautions apply to interpretations of the estimates of branching and phytomer emission probabilities. Our sample size is very limited: only 15 plants, as compared with the 250 plants measured by De Reffye (1981). Therefore, inter-plant variability is likely to produce important biases in the results, especially because the method relies on analytical expressions for the statistical distributions of the number of organs.

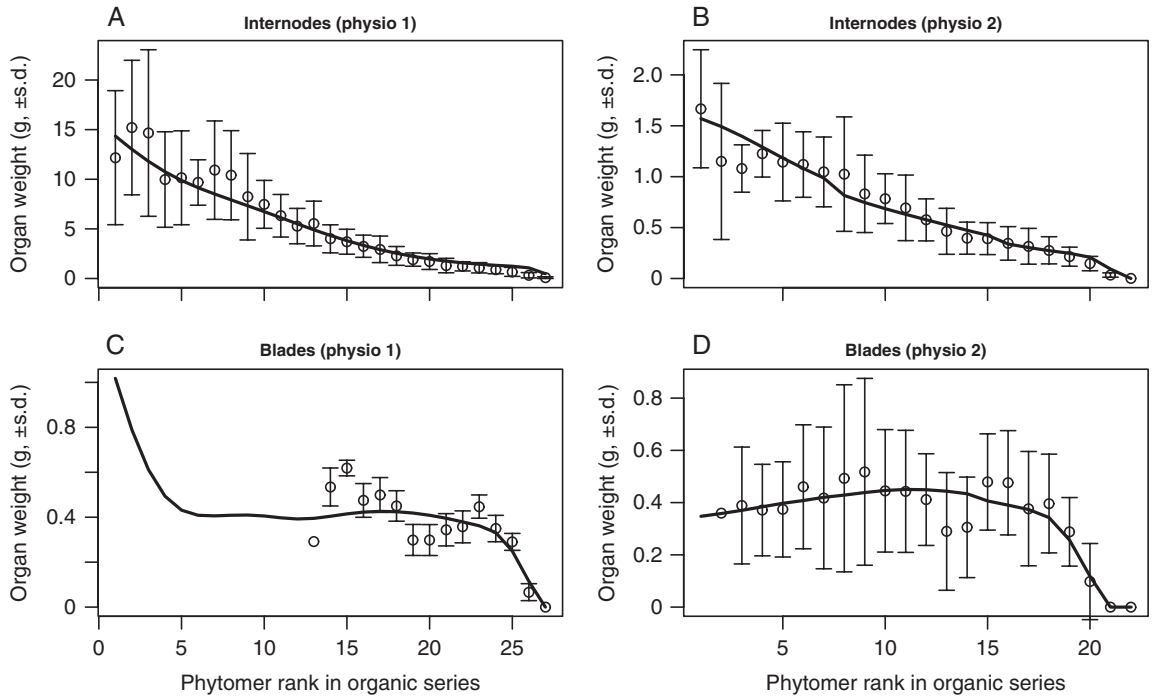

FIG. 7. Fitting organic series on the trunk (A, C) and on the branches (B, D) of *Coffea* with GreenLab ($R^2 = 0.95$ on $n = 81$ data). Girth growth is important on the trunk. First leaves on the trunk are missing because they have fallen, but for simulated data, all values are displayed to show the reconstructed weights of the first leaves (leaf weight is displayed even for senescent leaves).

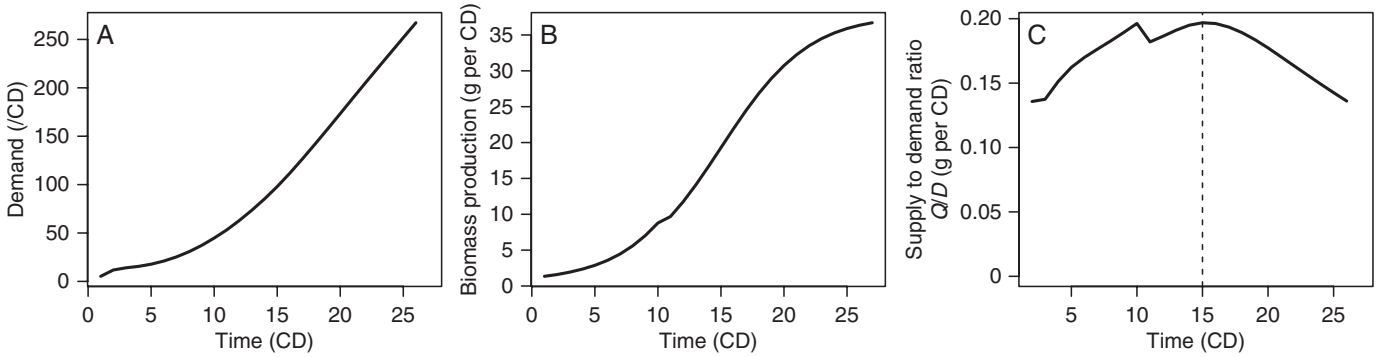

FIG. 8. Evolution of the demand (A) and biomass production (B) during growth of *Coffea*, as well as their ratio (C).

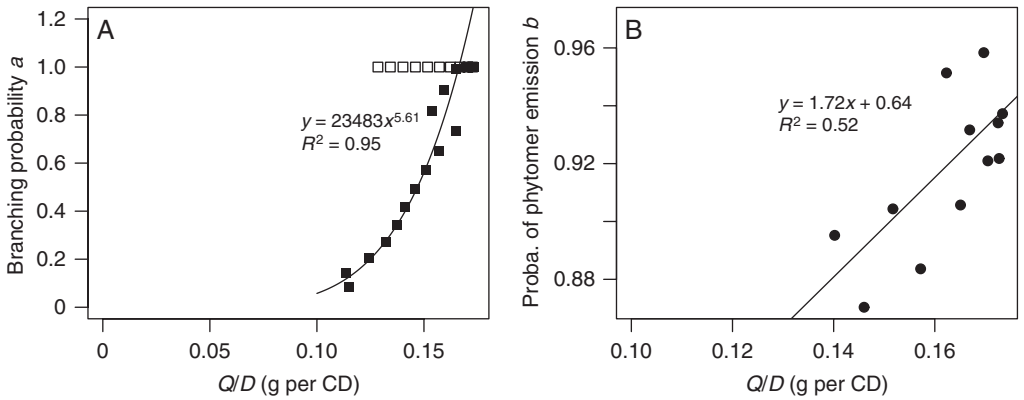

FIG. 9. Empirical relationship between *Q/D* and, respectively, bottom-up branching rate *a* (A) and development rate *b* (B). In A, open symbols represent the data corresponding to the phase with stabilization of the probabilities, not taken into account for the regression.

With all these sources of uncertainties in mind, we can use the results to address the question raised in the title of this paper: is internal trophic competition a relevant candidate for regulating plant development in plant growth models? Note that our point of view is here a pragmatic one, i.e. we simply question the relevance of using this variable to design a fully retro-active model that would behave like a plant: no causality is claimed nor any biological interpretation, and our tentative answer to that question is based on a statistical point of view.

Figure 9 provides mitigated conclusions to that question. The results seem very promising for the branching probability in the establishment phase ($t < 15$ CDs), with good correlation of this parameter with *Q/D*. Interestingly, *Q/D* reaches its maximum at about CD 15, close to the time when the branching probability stabilizes. Thus, in this establishment phase, the reconstructed source–sink dynamics are consistent with the model hypothesis that the source–sink ratio could have a regulatory role in plant development. However, after 15 CDs, the correlation no longer holds: the branching probability remains equal to 1 while *Q/D* decreases. This could be due to a hysteresis effect: once a threshold is reached, the system switches behaviour and another threshold value can provoke a new change. Here we expect that, after some period, the observed branching probability of these coffee trees would have decreased again. Indeed, De Reffye (1981) reported that the branching probability was 0.69 on older coffee trees (300 nodes were measured).

Regarding phytomer emission probability, no clear correlation was obtained, although a general trend could be observed. However, the amplitude of the variation of this parameter is far more limited than for the branching probability: b_h varies between just 0.87 and 0.96. So the effects of noise are likely to have much more impact especially with small sample sizes.

Despite these limitations, the full model with retroaction generates simulations that correctly reproduce the data on the average organic series. This is encouraging for pursuing further similar studies, especially as the resulting model gains in mechanistic degree.

Moreover, this result is in line with other studies using previous versions of GreenLab. Kang *et al.* (2011) found correlations between fruit-set probabilities and supply-to-demand ratio on tomato plants but the resulting relationship was not implemented in the model: fruit position was forced as observed. Mathieu *et al.* (2012) reported that periodic fruit-set patterns can be simulated in an FSPM when it is controlled by source–sink ratio: oscillations can be generated for certain ranges of parameter values, a pattern often observed in particular in fruit trees. Using a GL4-like model for grapevine but with an estimation procedure that relied for some part on a deterministic version of the model and that did not consider the average age of individual phytomers, Pallas *et al.* (2010) found that the rate of phytomer appearance according to thermal time was strongly affected by the plant's trophic status.

Generalizing this approach is hampered by the fact that this trophic competition is a non-measurable quantity that can be only assessed through estimation and that cannot be validated easily. Models such as GreenLab are therefore interesting in their role as 'source–sink solvers', i.e. as tools giving access to the internal trophic dynamics throughout growth. The probabilistic aspect nevertheless adds one more degree of complexity to the identification task and requires important methodological developments, as we have presented here. It is therefore expected that many further studies, based on experimental data collected on plants grown in controlled conditions, will be necessary to give a robust methodology and a consensual quantification of the trophic pressure. A promising avenue to explore

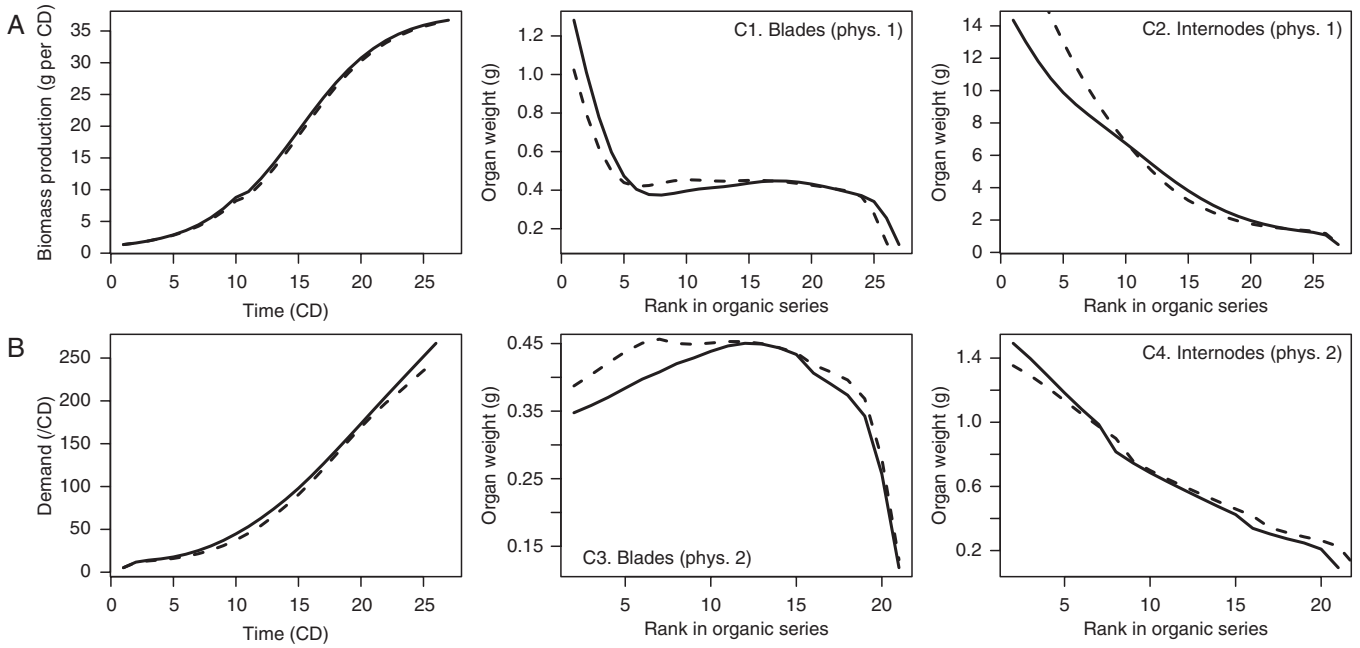

FIG. 10. Comparison of biomass production (A), demand (B) and organic series (C1–4) calculated by the 'GL2' stochastic model without retroaction (continuous lines) and that including the regulation of development probabilities by trophic pressure *Q/D* up to cycle 14 (dotted lines).

will then be to find measurable biological quantities that would be correlated to this *Q/D* variable: starch accumulation, for instance, or some other growth markers such as the pith diameter for the tropical genus *Cecropia* (our unpublished data).

Limitations and perspectives

The methodology developed for estimation of the 'GL4' model has the advantage of relying on a relatively light experimental protocol and our first *in silico* tests revealed correct results for the estimation (De Reffye *et al.*, 2018). Further tests are needed, especially by Monte-Carlo simulations with increasing sample sizes, to better quantify the accuracy of the estimation process. Indeed, even though the dataset can theoretically be built using only a few randomly sampled phytomers, in practice the large variability in both organ numbers and weights requires large sample sizes to provide reliable mean values. Such uncertainties should be better quantified by systematic analysis.

Clearly the ratio of biomass supply to demand is not the sole variable regulating plasticity of real plants. Environmental effects, and hormonal or biomechanical constraints also need to be taken into account. For instance, Pallas *et al.* (2010) found that a stochastic development model driven by trophic competition could reproduce more adequately their experimental datasets for grapevine when the additional influence of water stress was taken into account. Water is also a main influential variable for Coussement *et al.* (2018), who argue that plant growth can be sink-limited under water stress conditions. Inclusion of environmental variables could therefore be considered in our 'GL4' GreenLab version, as well as several modelling refinements, to provide added realism. The current simplified version has nevertheless many advantages that we have exploited in this study. In particular, as a 'toy-model', it provides a useful framework to test new methodologies such as the procedure of parameter estimation presented in the current paper. It is also interesting because its behaviour can be more easily understood and interpreted than complex 'blackbox' models and therefore helps to gain a good intuitive grasp of the different mechanisms at play in source–sink dynamics: complex emergent properties can already be simulated with basic processes owing to the feedback effect. Importantly, its further application to more real experimental data will allow us to investigate in more depth to what extent such source–sink mechanisms can explain or, at least, reproduce observed plant plasticity and variability.

ACKNOWLEDGEMENTS

We thank all those at Daolo station, especially Akaffou Sélastique and Legnaté Hyacinte, who helped with the acquisition of the experimental data used for this study.

LITERATURE CITED

Allen MT, Prusinkiewicz P, DeJong TM. 2005. Using Lsystems for modeling source–sink interactions, architecture and physiology of growing trees: the L-PEACH model. *New Phytologist* **166**: 869–880.

Barthélémy D, Caraglio Y. 2007. Plant architecture: a dynamic, multilevel and comprehensive approach to plant form, structure and ontogeny. *Annals of Botany* **99**: 375–407.

Brisson N, Gary C, Justes E, *et al*. 2003. An overview of the crop model STICS. *European Journal of Agronomy* **18**: 309–332.

Buis R, Barthou H. 1984. Relations dimensionnelles dans une série organique en croissance chez une plante supérieure. *Revue de Bio-Mathématiques* **85**: 1–19.

Chemouny S. 1997. *Estimation des paramètres du modèle de croissance et d'architecture végétale AMAPpara. Application au cotonnier taillé*. Master report, Université des sciences et techniques du Languedoc.

Combres JC, Pallas B, Rouan L, *et al*. 2013. Simulation of inflorescence dynamics in oil palm and estimation of environment-sensitive phenological phases: a model based analysis. *Functional Plant Biology* **40**: 263–279.

Costes E, Smith C, Renton M, Guédon Y, Prusinkiewicz P, Godin C. 2008. MAppleT: simulation of apple tree development using mixed stochastic and biomechanical models. *Functional Plant Biology* **35**: 936–950.

Cournède P, Letort V, Mathieu A, *et al*. 2011. Some parameter estimation issues in functional–structural plant modelling. *Mathematical Modelling of Natural Phenomena* **6**: 133–159.

Coussement JR, De Swaef T, Lootens P, Roldán-Ruiz I, Steppe K. 2018. Introducing turgor-driven growth dynamics into functional–structural plant models. *Annals of Botany* **121**: 849–861.

De Reffye P. 1981. Modèle mathématique aléatoire et simulation de la croissance et de l'architecture du caféier Robusta. 1ère partie. Étude du fonctionnement des méristèmes et de la croissance des axes végétatifs. *Café Cacao Thé* **25**: 83–104.

De Reffye P, Blaise F, Chemouny S, Jaffuel S, Fourcaud T, Houllier F. 1999. Calibration of a hydraulic architecture-based growth model of cotton plants. *Agronomie EDP Sciences* **19**: 265–280.

De Reffye P, Cognée M, Jaeger M, Traore B. 1988. Modélisation stochastique de la croissance et de l'architecture du cotonnier. 1. Tiges principales et branches fructifères primaires. *Coton et Fibres Tropicales* **43**: 269–291.

De Reffye P, Jaeger M, Sabatier S, Letort V. 2018. Modelling the interaction between functioning and organogenesis in a stochastic plant growth model: Methodology for parameter estimation and illustration. In: Louarn G, Song Y, eds. *IEEE Proceedings of 6th International Symposium on Plant Growth Modeling, Simulation, Visualization and Applications (PMA'18)*. Hefei, China: IEEE, 102–110.

Diao J, De Reffye P, Lei X, Guo H, Letort V. 2012. Simulation of the topological development of young eucalyptus using a stochastic model and sampling measurement strategy. *Computers and Electronics in Agriculture* **80**: 105–114.

Evers JB, Letort V, Renton M, Kang MZ. 2018. Computational botany: advancing plant science through functional–structural plant modelling. *Annals of Botany* **121**: 767–772.

Evers JB, Vos J, Yin X, Romero P, van der Putten PEL, Struik PC. 2010. Simulation of wheat growth and development based on organ-level photosynthesis and assimilate allocation. *Journal of Experimental Botany* **61**: 2203–2216.

Godin C, Caraglio Y. 1998. A multiscale model of plant topological structures. *Journal of Theoretical Biology* **191**: 1–46.

Griffon S, de Coligny F. 2014. AMAPstudio: an editing and simulation software suite for plants architecture modelling. *Ecological Modelling* **290**: 3–10.

Guo Y, Ma YT, Zhan ZG, *et al*. **2006.** Parameter optimization and field validation of the functional–structural model GREENLAB for maize. *Annals of Botany* **97**, 217–230

Hallé F, Oldeman R, Tomlinson P. 1978. *Tropical trees and forests, an architectural analysis*. New York: Springer.

Heuvelink E. 1995. Dry matter partitioning in a tomato plant: one common assimilate pool? *Journal of Experimental Botany* **46**: 1025–1033.

Kang M, Cournède PH, de Reffye P, Auclair D, Hu BG. 2008. Analytical study of a stochastic plant growth model: application to the GreenLab model. *Mathematics and Computers in Simulation* **78**: 57–75.

Kang MZ, Hua J, de Reffye P, Jaeger M. 2016. Parameter identification of plant growth models with stochastic development. In: Kang MZ, Evers J, Letort V, Renton M, eds. *2016 IEEE international conference on FunctionalStructural Plant Growth Modeling, Simulation, Visualization and Applications (FSPMA)*. Qingdao: IEEE, 98–105.

Kang M, Hua J, Wang X, de Reffye P, Jaeger M, Akaffou S. 2018. Estimating sink parameters of stochastic functional–structural plant models using organic series-continuous and rhythmic development. *Frontiers in Plant Science* **9**: 1688.

Kang MZ, Yang L, Zhang B, de Reffye P. 2011. Correlation between dynamic tomato fruit-set and source–sink ratio: a common relationship for different plant densities and seasons?. *Annals of Botany* **107**: 805–815.

Kurth W, Sloboda B. 1999. Tree and stand architecture and growth described by formal grammars. I. Non-sensitive trees. *Journal of Forest Science* **45**: 16–30.

Lehnebach R, Beyer R, Letort V, Heuret P. 2018. The pipe model theory half a century on: a review. *Annals of Botany* **121**: 773–795.

Lemaire S, Maupas F, Cournède PH, de Reffye P. 2009. A morphogenetic crop model for sugar-beet (*Beta vulgaris* L). In: Cao W, White JW, Wang E, eds. *Crop modeling and decision support*. Berlin: Springer, 116–129.

Letort V, Cournède PH, De Reffye P. 2010. Impact of topology on plant functioning: a theoretical analysis based on the greenlab model equations. In: Li GB, Jaeger M, Guo Y, eds. *Plant growth modeling, simulation, visualization and their Applications*. Washington: IEEE Computer Society, 341–348.

Letort V, Cournède PH, Mathieu A, de Reffye P, Constant T. 2008. Parameter identification of a functional–structural tree growth model and application to beech trees (*Fagus sylvatica*, Fagaceae). *Functional Plant Biology* **35**: 951–963.

Letort V, Sabatier S, Akaffou S, Hamon P, Hamon S, De Reffye P. 2012. Interspecific variability of biomass production of young *Coffea*: no influence of branch pruning. Experimental evidence and theoretical analysis. In: Kang MZ, Dumont Y, Guo Y, eds. *IEEE 4th international symposium on plant growth modeling, simulation, visualization and applications*. Shanghai, 224–227.

Lo E, Wang ZM, Lechowicz M, *et al*. 2001. Adaptation of the LIGNUM model for simulations of growth and light response in Jack pine. *Forest Ecology and Management* **150**: 279–291.

Loi C, Cournède PH. 2008. *Description of the GreenLab development model with stochastic L-systems and Monte-Carlo simulations. Technical report INRIA* Rocquencourt: INRIA.

Louarn G, Faverjon L. 2018. A generic individual-based model to simulate morphogenesis, C–N acquisition and population dynamics in contrasting forage legumes. *Annals of Botany* **121**: 875–896.

Luquet D, Dingkuhn M, Kim HK, Tambour L, Clement-Vidal A. 2006. EcoMeristem, a model of morphogenesis and competition among sinks in rice. 1. Concept, validation and sensitivity analysis. *Functional Plant Biology* **33**: 309–323.

Ma Y, Chen Y, Zhu J, *et al*. 2018. Coupling individual kernel-filling processes with source–sink interactions into GREENLAB-Maize. *Annals of Botany* **121**: 961–973.

Mathieu A, Cournède PH, Letort V, Barthelemy D, de Reffye P. 2009. A dynamic model of plant growth with interactions between development and functional mechanisms to study plant structural plasticity related to trophic competition. *Annals of Botany* **103**: 1173–1186.

Mathieu A, Letort V, Cournède PH, Zhang BG, Heuret P, de Reffye P. 2012. Oscillations in functional structural plant growth models. *Mathematical Modelling of Natural Phenomena* **7**: 47–66.

Okomas MP. 2018. *Modélisation de l'architecture et de la production de biomasse chez six espèces de caféiers (Coffea sp.) en Côté d'Ivoire*. PhD Thesis, Daola University.

Pallas P, Loi C, Christophe A, Cournède PH, Lecoeur J. 2010. Comparison of three approaches to model grapevine organogenesis in conditions of fluctuating temperature, solar radiation and soil water content. *Annals of Botany* **107**: 729–745.

Perttunen J, Sievänen R. 2005. Incorporating Lindenmayer systems for architectural development in a functional–structural tree model. *Ecological Modelling* **181**: 479–491.

Prusinkiewicz P, Lindenmayer A. 1990. *The algorithmic beauty of plants*. New York: Springer.

Sterck FJ, Schieving F, Lemmens A, Pons TL. 2005. Performance of trees in forest canopies: explorations with a bottom-up functional–structural plant growth model. *New Phytologist* **166**: 827–843.

Wang F, Kang MZ, Lu Q, *et al*. 2010. A stochastic model of tree architecture and biomass partitioning: application to Mongolian Scots pines. *Annals of Botany* **107**: 781–792.

Wu L, Le Dimet FX, de Reffye P, Hu BG, Cournède PH, Kang MZ. 2012. An optimal control methodology for plant growth – case study of water supply problem of sunflower. *Mathematics and Computers in Simulation* **82**: 909–923.

Yan H, Kang MZ, De Reffye P, Dingkuhn M. 2004. A dynamic, architectural plant model simulating resource-dependent growth. *Annals of Botany* **93**: 591–602.

Yin XY, Goudriaan J, Lantinga EA, Vos J, Spiertz HJ. 2003. A flexible sigmoid function of determinate growth. *Annals of Botany* **91**: 361–371.

Zhao X, de Reffye P, Xiong F, Hu B, Zhan Z. 2001. Dual-scale automaton model of virtual plant growth. *Chinese Journal of Computers* **24**: 608–615.